

# A crystalline doubly oxidized carbene

<https://doi.org/10.1038/s41586-023-06539-x>

Ying Kai Loh<sup>1</sup>✉, Mohand Melaimi<sup>1</sup>, Milan Gembicky<sup>1</sup>, Dominik Munz<sup>2</sup> & Guy Bertrand<sup>1</sup>✉

Received: 8 June 2023

Accepted: 14 August 2023

Published online: 20 September 2023

 Check for updates

The chemistry of carbon is governed by the octet rule, which refers to its tendency to have eight electrons in its valence shell. However, a few exceptions do exist, for example, the trityl radical ( $\text{Ph}_3\text{C}\cdot$ ) (ref. 1) and carbocation ( $\text{Ph}_3\text{C}^+$ ) (ref. 2) with seven and six valence electrons, respectively, and carbenes ( $\text{R}_2\text{C}\cdot$ )—two-coordinate octet-defying species with formally six valence electrons<sup>3</sup>. Carbenes are now powerful tools in chemistry, and have even found applications in material and medicinal sciences<sup>4</sup>. Can we undress the carbene further by removing its non-bonding electrons? Here we describe the synthesis of a crystalline doubly oxidized carbene ( $\text{R}_2\text{C}^{2+}$ ), through a two-electron oxidation/oxide-ion abstraction sequence from an electron-rich carbene<sup>5</sup>. Despite a cumulenic structure and strong delocalization of the positive charges, the dicoordinate carbon centre maintains significant electrophilicity, and possesses two accessible vacant orbitals. A two-electron reduction/deprotonation sequence regenerates the parent carbene, fully consistent with its description as a doubly oxidized carbene. This work demonstrates that the use of bulky strong electron-donor substituents can simultaneously impart electronic stabilization and steric protection to both vacant orbitals on the central carbon atom, paving the way for the isolation of a variety of doubly oxidized carbenes.

Carbenes constitute a class of neutral two-coordinate carbon species with six valence electrons. They violate the octet rule, a fundamental tenet governing main group elements. Since the discovery that strong  $\pi$  donor substituents permit their isolation under standard laboratory conditions<sup>6,7</sup>, stable carbenes have become powerful tools in the chemical and material sciences<sup>4</sup>.

Can we further deviate from the octet rule by removing one or two of the non-bonding electrons from the carbene centre? This would lead to either a radical cation or a doubly oxidized carbene. Early studies showed that the diphenylcarbene radical cation ( $\text{Ph}_2\text{C}^{\cdot+}$ ) can be transiently generated by single-electron oxidation of diazodiphenylmethane ( $\text{Ph}_2\text{CN}_2$ ) followed by  $\text{N}_2$  liberation, and could be spectroscopically characterized<sup>8–11</sup> (Fig. 1). More recently, several groups have explored the oxidation of N-heterocyclic carbenes (NHCs) and cyclic (alkyl) (amino)carbenes (CAACs) with various oxidants<sup>12–15</sup>. In all cases the reaction afforded the conjugate acid of carbenes. It was proposed that this was the result of the generation of the desired carbene radical cations that abstract  $\text{H}^{\cdot}$  from the solvent<sup>16</sup>. NHC radical cations have also been invoked as key intermediates in the emerging field of NHC single-electron transfer catalysis<sup>17,18</sup>.

Doubly oxidized carbenes ( $\text{R}_2\text{C}^{2+}$ ) are hitherto hypothetical species that have never been discussed in the literature. This might be due to the transient nature of the carbene radical cations, which decompose/react before the second oxidation could occur. Doubly oxidized carbenes possess two vacant orbitals around the dicoordinate carbon atom, rendering them isoelectronic with borinium ions ( $\text{R}_2\text{B}^+$ ) (refs. 19–21), an extremely electron-deficient class of boron cations<sup>22,23</sup>. However, doubly oxidized carbenes bear an extra positive charge, and thus they are expected to be substantially more electrophilic.

We recently demonstrated that an acyclic carbene bearing two strongly donating N-heterocyclic imine (NHI)<sup>24–26</sup> substituents features exceptional nucleophilicity, enabling the dearomatization of a proximal inert arene ring<sup>5</sup>. We reasoned that the electron-rich nature of the bis(imino)carbene, coupled with its flexible acyclic framework, is an ideal platform to access a doubly oxidized carbene. Here we report the synthesis and isolation of a crystalline dication derived from a bis(imino)carbene through a two-electron oxidation/oxide-ion abstraction strategy that bypasses the carbene radical cation.

## Synthesis and characterization of doubly oxidized carbene **1**<sup>2+</sup>

To bypass the generation of a carbene radical cation, we set out to explore an alternative strategy for the oxidation of bis(imino)carbene **1**. We envisaged a two-step approach, first by carbene coordination to a two-electron oxidant, then removing the oxidant along with two electrons. Accordingly, treating **1** with  $\text{I}_2$  as the two-electron oxidant formed the (iodo)carbenium ion as evidenced by *in situ*  $^1\text{H}$  nuclear magnetic resonance (NMR) (Fig. 2a and Supplementary Fig. 27)<sup>27</sup>. However, all attempts to abstract both iodides were unsuccessful, possibly due to the strong halophilicity of the target doubly oxidized carbene (vide infra). This prompted us to exchange the iodides for  $\text{O}^{2-}$ , which could be easily achieved through a one-pot procedure from **1**. Thus, treating **1** with  $\text{I}_2$  and then  $\text{NaOSiMe}_3$  afforded the neutral bis(imino) carbonyl compound **2** (ref. 28). Gratifyingly, subjecting **2** to triflic anhydride as the  $\text{O}^{2-}$  abstracting agent<sup>29</sup> led to a new species. The  $^1\text{H}$  NMR spectrum shows only one set of signals associated with the

<sup>1</sup>UCSD–CNRS Joint Research Laboratory (IRL 3555), Department of Chemistry and Biochemistry, University of California San Diego, La Jolla, CA, USA. <sup>2</sup>Coordination Chemistry, Saarland University, Saarbrücken, Germany. <sup>✉</sup>e-mail: yloh@ucsd.edu; gbertrand@ucsd.edu

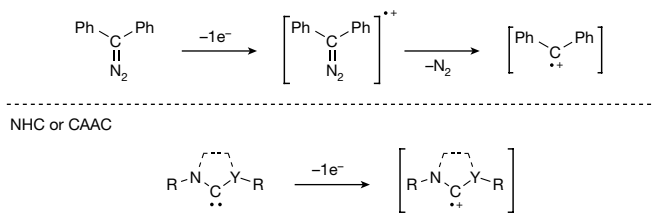


**Fig. 1 | Previous attempts at carbene oxidation.** The one-electron oxidation of diazo, NHC and CAAC derivatives led to non-isolable radical cations.

two NHI units. The central carbon signal appears at 119.8 ppm in the  $^{13}\text{C}\{^1\text{H}\}$  NMR, in excellent agreement with density-functional theory (DFT) calculations for the target dication  $\mathbf{1}^{2+}$  (PBE0/def2-TZVPP//r<sup>2</sup>SCAN-3c; 124.8 ppm). The  $^{19}\text{F}$  NMR spectrum shows only one signal at -77.9 ppm, which is in the typical range observed for an uncoordinated triflate anion.

Single-crystal X-ray diffraction analysis unambiguously confirmed that  $\mathbf{1}^{2+}[\text{TfO}]_2$  features a central two-coordinate carbon atom (Fig. 3a).  $\mathbf{1}^{2+}$  adopts an overall zigzag geometry in which the terminal CAACs are *cis*-bent. The central carbon C1 deviates slightly from linearity (163.2(4) $^\circ$ ) and the central C1–N1 and C1–N1' distances (mean, 1.197(2) Å) are within the range of  $\text{C}_{sp^2}$ –N double bonds. The adjacent nitrogen atoms (N1 and N1') subtend a more acute angle (147.8(3) $^\circ$ ), revealing a hybridization halfway between  $sp$  and  $sp^2$ . In addition, the terminal C2–N1 and C2'–N1' distances (mean, 1.349(3) Å) are midway between  $\text{C}_{sp^2}$ –N single and double bonds. These parameters indicate that the lone pairs on N1 and N1' are not only involved in  $\pi$  donation with central C1, but are also engaged in  $\pi$  back-bonding with the terminal CAAC carbon atoms (C2 and C2'). Strikingly, the terminal CAACs are almost orthogonal (79.6(2) $^\circ$ ) (Fig. 3b)—a distinct feature of even cumulenes<sup>30</sup>. In fact,  $\mathbf{1}^{2+}$  is isoelectronic with [4]cumulenes ( $\text{R}_2\text{C}=\text{C}=\text{C}=\text{C}\text{R}_2$ )<sup>31</sup>, and can be considered its dicationic nitrogen analogue ( $\mathbf{1}^{2+}\mathbf{b}$ ; Fig. 2c), accounting for the stability of  $\mathbf{1}^{2+}$ .

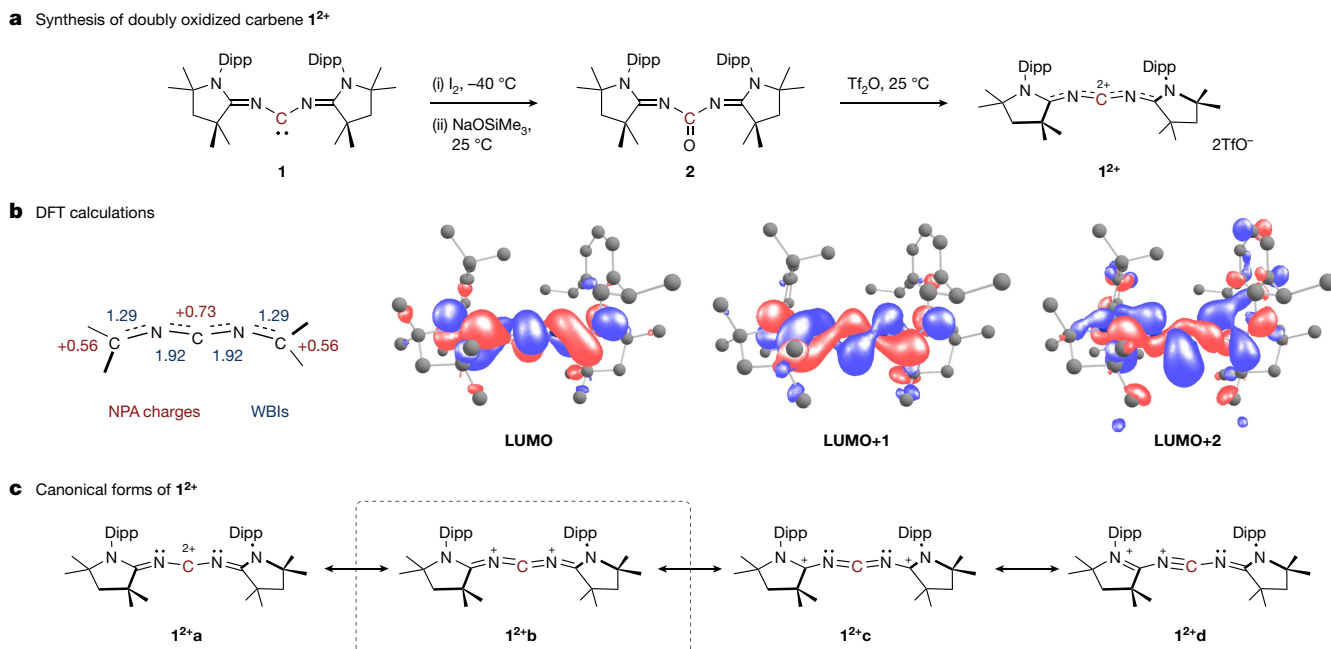
The two triflate anions in the outer sphere point directly at the central carbon C1 (mean S1–O1–C1 and S1'–O1'–C1 angle, 163.2(1) $^\circ$ ),

albeit from a considerable distance away (mean of C1–O1 and C1–O1', 3.020(3) Å) (Fig. 3a). This indicates that their approach to the central carbon is effectively impeded by the large steric profile of the flanking NHI substituents (for space-filling model, see Supplementary Table 1). These observations clearly indicate that the central C1 is the dominant electrophilic site.

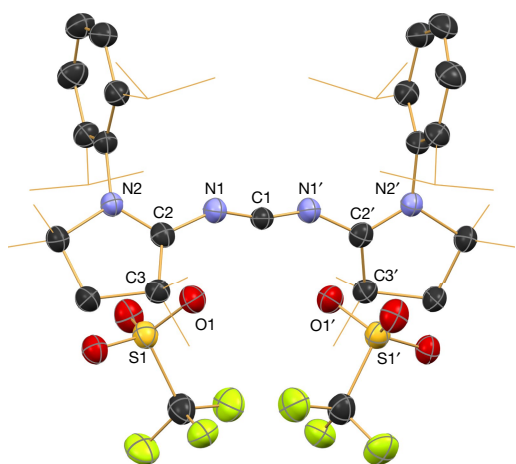
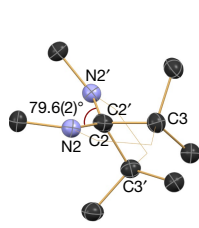
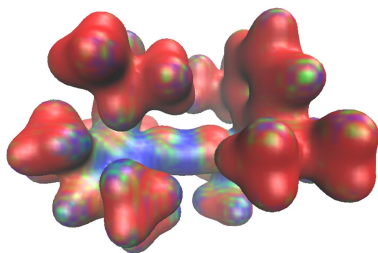
DFT calculations performed at the r<sup>2</sup>SCAN-3c level of theory accurately reproduced the structural parameters of  $\mathbf{1}^{2+}$ . Natural population analysis (NPA) reveals a large positive charge on the central C1 (+0.73), confirming that it is indeed the predominant electrophilic site of the molecule (Fig. 2b). This is also apparent from the electrostatic potential map (Fig. 3c). On the other hand, the peripheral C2 and C2' (+0.56) share some of the positive charge through allylic-type delocalization. Wiberg bond indices (WBIs) indicate double bond characters, albeit to a larger degree for the central C1–N1 and C1–N1' (mean, 1.92) than the terminal C2–N1 and C2'–N1' (mean, 1.29), consistent with an overall cumulene-type system with contiguous double bonds across the CNCNC unit (Fig. 2b). As for the molecular orbital picture, the LUMO and LUMO + 1 could be viewed as the orthogonal vacant  $p(\pi)$ -type orbitals on central C1, with contributions from C2 and C2' (Fig. 2b). Notably, these orbitals possess Möbius-type helicity, as with the frontier orbitals of [4]cumulenes (ref. 31), confirming the cumulenic nature of  $\mathbf{1}^{2+}$ . Interestingly, the LUMO + 2 bears a strong resemblance to the HOMO (lone pair orbital) of bis(imino)carbene  $\mathbf{1}$  (ref. 5), consistent with the notion that  $\mathbf{1}^{2+}$  is the doubly oxidized analogue of carbene  $\mathbf{1}$ .

The electronic structure of  $\mathbf{1}^{2+}$  could be illustrated by canonical forms  $\mathbf{1}^{2+}\mathbf{a}$  to  $\mathbf{1}^{2+}\mathbf{d}$  (Fig. 2c).  $\mathbf{1}^{2+}\mathbf{a}$  depicts a form in which both positive charges are purely localized on the central carbon, whereas  $\mathbf{1}^{2+}\mathbf{c}$  represents the opposite extreme in which the positive charges reside solely on the terminal CAAC carbon atoms. The unsymmetrical form  $\mathbf{1}^{2+}\mathbf{d}$  illustrates the slightly higher degree of multiple bonding for central C1–N1 than terminal C2–N1. On the basis of the structural parameters and DFT calculations, it is apparent that the electronic structure of  $\mathbf{1}^{2+}$  is highly delocalized<sup>32</sup> and resembles cumulenic  $\mathbf{1}^{2+}\mathbf{b}$ , which lies between the extremes of  $\mathbf{1}^{2+}\mathbf{a}$  and  $\mathbf{1}^{2+}\mathbf{c}$ .

We set out to assess the Lewis acidity of  $\mathbf{1}^{2+}$  by using a combination of fluoride ion affinity (FIA) and hydride ion affinity (HIA) to



**Fig. 2 | Synthesis and characterization of doubly oxidized carbene  $\mathbf{1}^{2+}$ .** **a**, Synthesis of  $\mathbf{1}^{2+}[\text{TfO}]_2$ . **b**, Calculated NPA charges (red), WBIs (blue), LUMO, LUMO + 1 and LUMO + 2. **c**, Canonical forms  $\mathbf{1}^{2+}\mathbf{a}$  to  $\mathbf{1}^{2+}\mathbf{d}$ . Dipp, 2,6-diisopropylphenyl.

**a** Solid-state structure of  $\mathbf{1}^{2+}[\text{TfO}^-]_2$ **b** End-on view (C2 to C2')**c** Electrostatic potential map**Fig. 3 | Doubly oxidized carbene  $\mathbf{1}^{2+}[\text{TfO}^-]_2$ .** **a**, Solid-state structure of  $\mathbf{1}^{2+}[\text{TfO}^-]_2$  (thermal ellipsoids set at 50% probability and H atoms omitted for clarity).

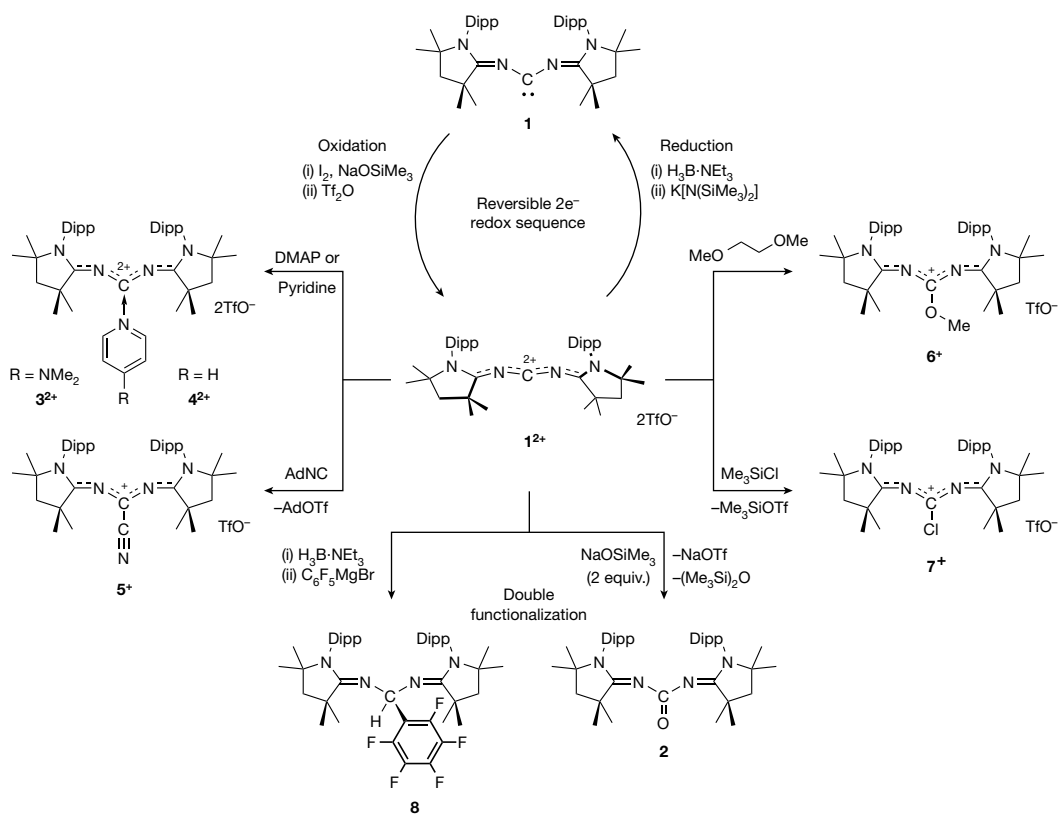
**b**, End-on view from C2 to C2' with N2–C2–C2'–N2' torsion angle labelled.

**c**, Electrostatic potential map (blue, electron depletion; red, electron excess).

gauge its hard and soft Lewis acidity, respectively<sup>33</sup>. The calculated gas-phase affinities for  $\mathbf{1}^{2+}$  (FIA, 890 kJ mol<sup>-1</sup>; HIA, 1,066 kJ mol<sup>-1</sup>) reflect the softer nature of the central carbon. Notably, these values exceed those of trityl carbocation  $\text{Ph}_3\text{C}^+$  (FIA, 664 kJ mol<sup>-1</sup>; HIA, 847 kJ mol<sup>-1</sup>)<sup>32</sup>, which is the archetypical carbon Lewis acid. When compared with other p-block element Lewis acids, we find that the affinities for  $\mathbf{1}^{2+}$  fall between those of the isoelectronic bis(imino) borinium ion ( $^3\text{Bu}_3\text{PN}_2\text{B}^+$ ) (FIA, 599 kJ mol<sup>-1</sup>; HIA, 569 kJ mol<sup>-1</sup>)<sup>19</sup>, which also features an extended cumulenic structure, and the Lewis super acid ( $\text{Cp}^*\text{P}^{2+}$ ) (FIA, 1,170 kJ mol<sup>-1</sup>; HIA, 1,238 kJ mol<sup>-1</sup>)<sup>34</sup>. In fact, they are comparable to those of tris(imino)phosphorus(V) dication ( $\text{NHC}=\text{N}_3\text{P}^{2+}$ ) (FIA, 909 kJ mol<sup>-1</sup>; HIA, 933 kJ mol<sup>-1</sup>)<sup>35</sup>. Notably, we obtained the same trend when dichloromethane solvation was considered in the calculations (Supplementary Table 7). Overall, this assessment indicates that  $\mathbf{1}^{2+}$  maintains a substantial Lewis acidity, despite cumulenic stabilization.

### Reactivity of doubly oxidized carbene $\mathbf{1}^{2+}$

We turned our attention to explore the reactivity of  $\mathbf{1}^{2+}$ . Subjecting  $\mathbf{1}^{2+}$  to neutral Lewis bases dimethylaminopyridine (DMAP) and even pyridine afforded base-stabilized dication  $\mathbf{3}^{2+}$  and  $\mathbf{4}^{2+}$ , respectively (Fig. 4), confirming that the central dicoordinate carbon is indeed the dominant electrophilic site of the molecule. Surprisingly, using 1-adamantyl isocyanide results in the formation of (cyano)carbenium ion  $\mathbf{5}^+$  (Fig. 4) and 1-adamantyl triflate. We surmised that the initial coordination of 1-adamantyl isocyanide to  $\mathbf{1}^{2+}$  forms a highly electron-deficient nitrilium dication, which fragments into  $\mathbf{5}^+$  and 1-adamantyl carbocation<sup>36</sup>, as the corresponding  $\text{S}_{\text{N}}2$  pathway is not permitted. Overall, this can be considered as a transfer of  $\text{CN}^-$  from an aliphatic carbocation<sup>37</sup> to  $\mathbf{1}^{2+}$ , reflecting the strong electrophilicity of the latter.

**Fig. 4 | Reactivity of doubly oxidized carbene  $\mathbf{1}^{2+}$  and a reversible  $\mathbf{1}/\mathbf{1}^{2+}$  redox system.**  $\mathbf{1}^{2+}$  can undergo addition of neutral bases (DMAP and pyridine); abstraction of  $\text{CN}^-$  from 1-adamantyl isocyanide,  $\text{MeO}^-$  from dimethoxyethane

and  $\text{Cl}^-$  from  $\text{Me}_3\text{SiCl}$ ; double functionalization with  $\text{H}^+/\text{C}_6\text{F}_5^-$  and  $\text{O}^{2-}$ ;  $\mathbf{1}^{2+}$  can participate in a reversible two-electron redox process with carbene **1**. Ad, 1-adamantyl; equiv., equivalents.

Motivated by this finding, we then investigated the anion abstracting ability of  $\mathbf{1}^{2+}$ . It can abstract  $\text{MeO}^-$  from dimethoxyethane and  $\text{Cl}^-$  from  $\text{Me}_3\text{SiCl}$  to form carbenium ions  $\mathbf{6}^+$  and  $\mathbf{7}^+$ , respectively (Fig. 4), showcasing its strong oxophilic and halophilic nature. The latter observation stands in marked contrast to the borinium ion  $(^3\text{Bu}_3\text{PN})_2\text{B}^+$  (ref. 19), which spontaneously ejects  $\text{Cl}^-$ , consistent with the stronger halophilicity of  $\mathbf{1}^{2+}$  as predicted by FIA measurements.

Having established that the central carbon of  $\mathbf{1}^{2+}$  is the dominant electrophilic site for the initial nucleophilic attack, we were curious to ascertain the position for which a second nucleophile would react. With this in mind, we first treated  $\mathbf{1}^{2+}$  with  $\text{H}^-$  (via  $\text{H}_3\text{B} \cdot \text{NEt}_3$ ), and subsequently with  $\text{C}_6\text{F}_5^-$  (via  $\text{C}_6\text{F}_5\text{MgBr}$ ), and observed the formation of the neutral compound  $\mathbf{8}$  (Fig. 4).  $\mathbf{8}$  features both nucleophilic components on its central carbon, confirming the presence of two accessible coordination sites on the dicoordinate carbon centre of  $\mathbf{1}^{2+}$ . In fact,  $\mathbf{8}$  can also be attained via the reaction of parent bis(imino)carbene  $\mathbf{1}$  with  $\text{C}_6\text{F}_5\text{H}$  (ref. 5), fully consistent with the description of  $\mathbf{1}^{2+}$  as doubly oxidized bis(imino)carbene. Next, we wondered whether the central carbon of  $\mathbf{1}^{2+}$  can also engage in a double bond. Using  $\text{NaOSiMe}_3$  as  $\text{O}^{2-}$  transfer reagent afforded the neutral bis(imino)carbonyl compound  $\mathbf{2}$  (Fig. 4), further corroborating the existence of both vacant orbitals on the central carbon.

## Reversible $\mathbf{1}/\mathbf{1}^{2+}$ redox system

Reversible two-electron redox processes are the hallmark of transition metal catalysis. In stark contrast, main group p-block compounds rarely exhibit such processes<sup>38–40</sup>. Having established that bis(imino)carbene  $\mathbf{1}$  can undergo a two-electron oxidation sequence giving  $\mathbf{1}^{2+}$  (Fig. 4), we set out to explore the reverse two-electron reduction by using a similar two-step strategy. We reasoned that this could be achieved by first using  $\text{H}^-$  as the two-electron reductant, then removing  $\text{H}^+$  and leaving behind two electrons. Accordingly, subjecting  $\mathbf{1}^{2+}$  to  $\text{H}_3\text{B} \cdot \text{NEt}_3$  afforded the protonated bis(imino)carbene, which could be deprotonated by  $\text{K}[\text{N}(\text{SiMe}_3)_2]$ , leading to the successful regeneration of  $\mathbf{1}$ . Hence,  $\mathbf{1}/\mathbf{1}^{2+}$  constitutes an unprecedented reversible two-electron redox system between a carbene and its doubly oxidized counterpart<sup>41</sup>. More importantly, this is a further demonstration that  $\mathbf{1}^{2+}$  behaves as a doubly oxidized carbene.

## Conclusion

More than 30 years after the discovery of a stable carbene<sup>6</sup>, this work shows that a doubly oxidized carbene can be isolated as well. In his Nobel lecture, Olah stated, “it should be clear that in carbocationic systems, varying degrees of delocalization always exist”<sup>42</sup>. Despite the cumulenic delocalization of the positive charges,  $\mathbf{1}^{2+}$  shows substantial electrophilicity at the dicoordinate carbon centre. It is amenable to two successive nucleophilic attacks, in line with the existence of two accessible coordination sites at the central carbon. We also show that it can participate in an unprecedented reversible two-electron redox system with parent bis(imino)carbene, fully consistent with its description as a doubly oxidized bis(imino)carbene. This work demonstrates that bulky strong electron-donor substituents can be used both to mask vacant orbitals at the central carbon atom and to prevent the two anions from coordination, paving the way for the isolation of a variety of doubly oxidized carbenes.

## Online content

Any methods, additional references, Nature Portfolio reporting summaries, source data, extended data, supplementary information, acknowledgements, peer review information; details of author contributions and competing interests; and statements of data and code availability are available at <https://doi.org/10.1038/s41586-023-06539-x>.

1. Gomberg, M. An instance of trivalent carbon: triphenylmethyl. *J. Am. Chem. Soc.* **22**, 757–771 (1900).
2. Grützmacher, H. & Marchand, C. M. Heteroatom stabilized carbenium ions. *Coord. Chem. Rev.* **163**, 287–344 (1997).
3. Bourissou, D., Guerret, O., Gabbaï, F. P. & Bertrand, G. Stable carbenes. *Chem. Rev.* **100**, 39–91 (2000).
4. Bellotti, P., Koy, M., Hopkinson, M. N. & Glorius, F. Recent advances in the chemistry and applications of N-heterocyclic carbenes. *Nat. Rev. Chem.* **5**, 711–725 (2021).
5. Loh, Y. K., Melaimi, M., Munz, D. & Bertrand, G. An air-stable “masked” bis(imino)carbene: a carbon-based dual ambiphile. *J. Am. Chem. Soc.* **145**, 2064–2069 (2023).
6. Igau, A., Grützmacher, H., Baceiredo, A. & Bertrand, G. Analogous  $\alpha,\alpha'$ -bis-carbenoid triply bonded species: synthesis of a stable  $\lambda^3$ -phosphinocarbene– $\lambda^3$ -phosphaacetylene. *J. Am. Chem. Soc.* **110**, 6463–6466 (1988).
7. Arduengo, A. J. III, Harlow, R. L. & Kline, M. A stable crystalline carbene. *J. Am. Chem. Soc.* **113**, 361–363 (1991).
8. Parker, V. D. & Bethell, D. Carbene cation radicals: the kinetics of their formation from diazoalkane cation radicals and their reactions. *J. Am. Chem. Soc.* **109**, 5066–5072 (1987).
9. Bethell, D. & Parker, V. D. In search of carbene ion radicals in solution: reaction pathways and reactivity of ion radicals of diazo compounds. *Acc. Chem. Res.* **21**, 400–407 (1988).
10. Bally, T., Matzinger, S. & Truttmann, L. Diphenyl carbene cation: electronic and molecular structure. *J. Am. Chem. Soc.* **115**, 7007–7008 (1993).
11. Stoub, D. & Goodman, G. V. Diarylcarbene cation radicals: generation and chemical reactivity in solution. *J. Am. Chem. Soc.* **119**, 11110–11111 (1997).
12. Rammal, T., McKenzie, I., Gorodetsky, B., Tsang, E. M. W. & Clyburne, J. A. C. Reactions of N-heterocyclic carbenes (NHCs) with one-electron oxidants: possible formation of a carbene cation radical. *Chem. Commun.* 1054–1055 (2004).
13. Dong, Z. et al. SET processes in Lewis acid–base reactions: the tritylation of N-heterocyclic carbenes. *Chem. Sci.* **11**, 7615–7618 (2020).
14. Shaikh, A. C., Veleta, J. M., Moutet, J. & Gianetti, T. L. Triaoxatriangulenium (TOTA<sup>+</sup>) as a robust carbon-based Lewis acid in frustrated Lewis pair chemistry. *Chem. Sci.* **12**, 4841–4849 (2021).
15. Maiti, A. et al. Disclosing cyclic(alkyl)(amino)carbenes as one-electron reductants: synthesis of acyclic(amino)(aryl)carbene-based Kekulé diradicaloids. *Chem. Eur. J.* **28**, e2020104567 (2022).
16. Song, H. & Lee, E. Revisiting the reaction of iPr with tritylium: an alternative mechanistic pathway. *Chem. Eur. J.* **29**, e202203364 (2023).
17. Zhang, Q., Lei, H., Zhou, C.-Y. & Wang, C. Construction of N-polyheterocycles by N-heterocyclic carbene catalysis via a regioselective intramolecular radical addition/cyclization cascade. *Org. Lett.* **24**, 4615–4619 (2022).
18. Liu, L., Zhang, Q. & Wang, C. Redox-neutral generation of iminyl radicals by N-heterocyclic carbene catalysis: rapid access to phenanthridines from vinyl azides. *Org. Lett.* **24**, 5913–5917 (2022).
19. Courtenay, S., Mutus, J. Y., Schurko, R. W. & Stephan, D. W. The extended borinium cation:  $[(^3\text{Bu}_3\text{PN})_2\text{B}]^+$ . *Angew. Chem. Int. Ed.* **41**, 498–501 (2002).
20. Shoji, Y., Tanaka, N., Mikami, K., Uchiyama, M. & Fukushima, T. A two-coordinate boron cation featuring C–B–C bonding. *Nat. Chem.* **6**, 498–503 (2014).
21. Bamford, K. L., Qu, Z.-W. & Stephan, D. W. Activation of  $\text{H}_2$  and  $\text{Et}_3\text{SiH}$  by the borinium cation  $[\text{MesB}^2]^-$ : avenues to cations  $[\text{MesB}(\mu\text{-H})_2(\mu\text{-Mes})\text{BMes}]^+$  and  $[\text{H}_2\text{B}(\mu\text{-H})(\mu\text{-Mes})\text{B}(\mu\text{-Mes})(\mu\text{-H})\text{BH}_3]^-$ . *J. Am. Chem. Soc.* **141**, 6180–6184 (2019).
22. Franz, D. & Inoue, S. Cationic complexes of boron and aluminum: an early 21st century viewpoint. *Chem. Eur. J.* **25**, 2898–2926 (2018).
23. Piers, W. E., Bourke, S. C. & Conroy, K. C. Borinium, boreonium, and boronium ions: synthesis, reactivity, and applications. *Angew. Chem. Int. Ed.* **44**, 5016–5036 (2005).
24. Ochiai, T., Franz, D. & Inoue, S. Applications of N-heterocyclic imines in main group chemistry. *Chem. Soc. Rev.* **45**, 6327–6344 (2016).
25. Goettel, J. T., Gao, H., Dotzauer, S. & Braunschweig, H.  $^{\text{Me}}\text{CAAC}=\text{N}^+$ : a cyclic (alkyl)(amino)carbene imino ligand. *Chem. Eur. J.* **26**, 1136–1143 (2020).
26. Huynh, S. et al. Cyclic alkyl(amino)imimates (CAAl) as strong 2*o*,4*π*-electron donor ligands for the stabilisation of boranes and diboranes(4): a synthetic and computational study. *Dalton Trans.* **52**, 3869–3876 (2023).
27. Pal, S., Manae, M. A., Khade, V. V. & Khan, S. Reactivity of N-heterocyclic carbene, 1,3-bis(2,6-diisopropylphenyl)imidazol-2-ylidene, towards heavier halogens ( $\text{Br}_2$  and  $\text{I}_2$ ). *J. Indian Chem. Soc.* **95**, 765–770 (2018).
28. Loh, Y. K., Fuentes, M. Á., Vasko, P. & Aldridge, S. Successive protonation of an N-heterocyclic imine derived carbonyl: superelectrophilic dication versus masked acylium ion. *Angew. Chem. Int. Ed.* **57**, 16559–16563 (2018).
29. Loh, Y. K. et al. An acid-free anionic oxaborane isoelectronic with carbonyl: facile access and transfer of a terminal B=O double bond. *J. Am. Chem. Soc.* **141**, 8073–8077 (2019).
30. Januszewski, J. A. & Tykwiński, R. R. Synthesis and properties of long  $[n]$ -cumulenes ( $n \geq 5$ ). *Chem. Soc. Rev.* **43**, 3184–3203 (2014).
31. Pinter, P. & Munz, D. Controlling möbius-type helicity and the excited-state properties of cumulenes with carbenes. *J. Phys. Chem. A* **124**, 10100–10110 (2020).
32. Couchman, S. A., Wilson, D. J. D. & Dutton, J. L. Is the perfluorinated triyl cation worth a revisit? A theoretical study on the Lewis acidities and stabilities of highly halogenated triyl derivatives. *Eur. J. Org. Chem.* 3902–3908 (2014).
33. Jupp, A. R., Johnstone, T. C. & Stephan, D. W. The global electrophilicity index as a metric for Lewis acidity. *Dalton Trans.* **47**, 7029–7035 (2018).
34. Zhou, J., Liu, L. L., Cao, L. L. & Stephan, D. W. A phosphorus Lewis super acid:  $\text{η}^5\text{-pentamethylcyclopentadienyl phosphorus dication}$ . *Chem. 4*, 2699–2708 (2018).
35. Mehlmann, P., Witteler, T., Wilm, L. F. B. & Dielmann, F. Isolation, characterization and reactivity of three-coordinate phosphorus dication isoelectronic to alanes and silylum cations. *Nat. Chem.* **11**, 1139–1143 (2019).

---

36. Olah, G. et al. Bridgehead adamantyl, diamantyl, and related cations and dications. *J. Am. Chem. Soc.* **107**, 2764–2772 (1985).
37. Kato, T. & Reed, C. A. Putting tert-butyl cation in a bottle. *Angew. Chem. Int. Ed.* **43**, 2908–2911 (2004).
38. Légaré, M.-A., Pranckevicius, C. & Braunschweig, H. Metallomimetic chemistry of boron. *Chem. Rev.* **119**, 8231–8261 (2019).
39. Weetman, S. & Inoue, S. The road travelled: after main-group elements as transition metals. *ChemCatChem* **10**, 4213–4228 (2018).
40. Martin, D., Melaimi, M., Soleilhavoup, M. & Bertrand, G. Stable singlet carbenes as mimics for transition metal centers. *Chem. Sci.* **2**, 389–399 (2011).
41. Lipshultz, J. M., Li, G. & Radosevich, A. T. Main group redox catalysis of organopnictogens: vertical periodic trends and emerging opportunities in group 15. *J. Am. Chem. Soc.* **143**, 1699–1721 (2021).
42. Olah, G. A. My search for carbocations and their role in chemistry (Nobel lecture). *Angew. Chem. Int. Ed.* **34**, 1393–1405 (1995).

**Publisher's note** Springer Nature remains neutral with regard to jurisdictional claims in published maps and institutional affiliations.

Springer Nature or its licensor (e.g. a society or other partner) holds exclusive rights to this article under a publishing agreement with the author(s) or other rightsholder(s); author self-archiving of the accepted manuscript version of this article is solely governed by the terms of such publishing agreement and applicable law.

© The Author(s), under exclusive licence to Springer Nature Limited 2023

## Methods

### General considerations

All manipulations were carried out using standard Schlenk line or dry-box techniques under an atmosphere of argon. Solvents were dried over sodium benzophenone ketyl or calcium hydride, degassed and stored over activated molecular sieves or K mirror. Mass spectra were performed at the UC San Diego Mass Spectrometry Laboratory on an Agilent 6230 Accurate-Mass TOFMS spectrometer. NMR spectra were recorded on a Jeol 400 ( $^1\text{H}$ , 400 MHz;  $^{13}\text{C}$ , 101 MHz;  $^{19}\text{F}$ , 376 MHz) spectrometer, at ambient temperature unless otherwise noted. Chemical shift values for  $^1\text{H}$  are referenced to the residual protio-solvent ( $^1\text{H}$ ) resonance of  $\text{CDCl}_3$  ( $\delta$ , 7.26),  $\text{C}_6\text{D}_6$  ( $\delta$ , 7.16). Chemical shift values for  $^{13}\text{C}$  are referenced to the solvent ( $^{13}\text{C}$ ) resonance of  $\text{CDCl}_3$  ( $\delta$ , 77.16),  $\text{C}_6\text{D}_6$  ( $\delta$ , 128.06). Chemical shift values for  $^{19}\text{F}$  are referenced to  $\text{CFCl}_3$  ( $\delta$ , 19). Chemical shifts are quoted in  $\delta$  (ppm) and coupling constants in  $J$  (Hz). NMR multiplicities are abbreviated as follows: s, singlet; d, doublet; t, triplet; sept, septet; m, multiplet; brs, broad signal. Assignments were confirmed using two-dimensional  $^1\text{H}$ – $^1\text{H}$  and  $^{13}\text{C}$ – $^1\text{H}$  NMR correlation experiments. Single-crystal X-ray diffraction data were collected on Bruker Apex diffractometers using Mo  $\text{K}\alpha$  radiation ( $\lambda = 0.71073 \text{ \AA}$ ) or Cu  $\text{K}\alpha$  radiation ( $\lambda = 1.54178 \text{ \AA}$ ) at the UC San Diego Crystallography Facility.

### Starting materials

[( $^{\text{Me}}\text{CAACN}$ )<sub>2</sub> $\text{CH}^+$ ][ $\text{TfO}^-$ ] (ref. 5) and  $^{\text{Me}}\text{CAACN}(\text{SiMe}_3)$  (ref. 25) were prepared according to literature procedures. All other reagents were purchased from commercial sources and used without further purification unless otherwise noted.

**Preparation of **2**.** A mixture of [( $^{\text{Me}}\text{CAACN}$ )<sub>2</sub> $\text{CH}^+$ ][ $\text{TfO}^-$ ] (90 mg, 0.12 mmol) and  $\text{K}[\text{N}(\text{SiMe}_3)_2]$  (24 mg, 0.12 mmol) in a vial was cooled to  $-40^\circ\text{C}$  in the glovebox. Tetrahydrofuran (THF) (3 ml) at  $-40^\circ\text{C}$  was added to the mixture to form an orange-red solution, which was stirred for 5 min.  $\text{I}_2$  (30 mg, 0.12 mmol) was added, and the resulting mixture was allowed to stir for a further 5 min before warming up to room temperature.  $\text{NaOSiMe}_3$  (27 mg, 0.24 mmol) was added, and the mixture stirred overnight at room temperature. The mixture was filtered, and the filtrate dried under vacuum. The filtrate was redissolved in benzene (2 ml) and filtered. The filtrate was then dried under vacuum to yield **2** (19 mg, 26% yield) as a light yellow powder. Single crystals suitable for X-ray crystallography were obtained by evaporation from a benzene solution at room temperature. Alternative synthesis of **2** from  $1^{2+}[\text{TfO}^-]_2$ : To a mixture of  $1^{2+}[\text{TfO}^-]_2$  (460 mg, 0.50 mmol) and  $\text{NaOSiMe}_3$  (114 mg, 1.0 mmol) was added benzene (5 ml) and sonicated overnight. The suspension was then filtered and the filtrate dried under vacuum to yield **2** (199 mg, 63% yield) as a light yellow powder. Alternative synthesis of **2** from  $^{\text{Me}}\text{CAACN}(\text{SiMe}_3)$ : To a mixture of  $^{\text{Me}}\text{CAACN}(\text{SiMe}_3)$  (957 mg, 2.57 mmol) and  $(\text{COCl})_3$  (137 mg, 0.43 mmol) was added benzene (3 ml) and stirred overnight. The suspension was then filtered and the filtrate dried under vacuum to yield **2** (598 mg, 75% yield) as a light yellow powder.  $^1\text{H}$  NMR (400 MHz,  $\text{CDCl}_3$ ,

297 K):  $\delta = 1.15$  (s, 12H,  $\text{C}(\text{CH}_3)_2$ ), 1.16 (d,  $^3J_{\text{HH}} = 6.5 \text{ Hz}$ , 12H,  $\text{CH}(\text{CH}_3)_2$ ), 1.23 (d,  $^3J_{\text{HH}} = 6.9 \text{ Hz}$ , 12H,  $\text{CH}(\text{CH}_3)_2$ ), 1.29 (s, 12H,  $\text{C}(\text{CH}_3)_2$ ), 1.94 (s, 4H,  $\text{CH}_2$ ), 3.02 (sept,  $^3J_{\text{HH}} = 6.7 \text{ Hz}$ , 4H,  $\text{CH}(\text{CH}_3)_2$ ), 7.15 (d,  $^3J_{\text{HH}} = 7.7 \text{ Hz}$ , 4H, Dipp-*m*-CH), 7.25 (t,  $^3J_{\text{HH}} = 7.6 \text{ Hz}$ , 2H, Dipp-*p*-CH).  $^{13}\text{C}\{\text{H}\}$  NMR (101 MHz,  $\text{CDCl}_3$ , 297 K):  $\delta = 23.2$  ( $\text{CH}(\text{CH}_3)_2$ ), 26.7 ( $\text{CH}(\text{CH}_3)_2$ ), 28.7 ( $\text{C}(\text{CH}_3)_2$ ), 29.0 ( $\text{CH}(\text{CH}_3)_2$ ), 29.4 ( $\text{C}(\text{CH}_3)_2$ ), 43.1 ( $\text{C}(\text{CH}_3)_2$ ), 54.5 ( $\text{CH}_2$ ), 61.7 ( $\text{C}(\text{CH}_3)_2$ ), 123.7 (Dipp-*m*-CH), 127.9 (Dipp-*p*-CH), 132.7 (Dipp-*i*-C), 149.0 (Dipp-*o*-C), 164.5 ( $\text{C}_{\text{CAAC}}$ ), 167.7 (CO). High-resolution mass spectrometry (HRMS) ( $m/z$ ): [M + H]<sup>+</sup> calculated for  $\text{C}_{41}\text{H}_{63}\text{N}_4\text{O}$ , 627.4996; found, 627.5002.

**Preparation of  $1^{2+}[\text{TfO}^-]_2$ .** To **2** (600 mg, 0.96 mmol) in benzene (6 ml) was added trifluoromethanesulfonic anhydride (0.48 ml, 2.9 mmol) dropwise while stirring at room temperature. The orange solution turned dark brown with concomitant formation of a white precipitate. After stirring for a further 5 min, the suspension was filtered off and the residue dried under vacuum to yield  $1^{2+}[\text{TfO}^-]_2$  (832 mg, 89% yield) as an off-white powder. Single crystals suitable for X-ray crystallography were obtained by slow evaporation from a concentrated chloroform solution at room temperature.  $^1\text{H}$  NMR (400 MHz,  $\text{CDCl}_3$ , 297 K):  $\delta = 1.03$  (d,  $^3J_{\text{HH}} = 6.6 \text{ Hz}$ , 12H,  $\text{CH}(\text{CH}_3)_2$ ), 1.32 (d,  $^3J_{\text{HH}} = 6.6 \text{ Hz}$ , 12H,  $\text{CH}(\text{CH}_3)_2$ ), 1.52 (s, 12H,  $\text{C}(\text{CH}_3)_2$ ), 1.80 (s, 12H,  $\text{C}(\text{CH}_3)_2$ ), 2.62 (s, 4H,  $\text{CH}_2$ ), 2.74 (sept,  $^3J_{\text{HH}} = 6.6 \text{ Hz}$ , 4H,  $\text{CH}(\text{CH}_3)_2$ ), 7.32 (d,  $^3J_{\text{HH}} = 7.9 \text{ Hz}$ , 4H, Dipp-*m*-CH), 7.52 (t,  $^3J_{\text{HH}} = 7.8 \text{ Hz}$ , 2H, Dipp-*p*-CH).  $^{13}\text{C}\{\text{H}\}$  NMR (101 MHz,  $\text{CDCl}_3$ , 297 K):  $\delta = 22.7$  ( $\text{CH}(\text{CH}_3)_2$ ), 26.8 ( $\text{CH}(\text{CH}_3)_2$ ), 27.4 ( $\text{C}(\text{CH}_3)_2$ ), 28.2 ( $\text{C}(\text{CH}_3)_2$ ), 29.6 ( $\text{CH}(\text{CH}_3)_2$ ), 47.8 ( $\text{CH}_2$ ), 49.7 ( $\text{C}(\text{CH}_3)_2$ ), 79.1 ( $\text{C}(\text{CH}_3)_2$ ), 119.8 ( $\text{C}_{\text{central}}$ ), 120.9 (q,  $^1J_{\text{CF}} = 286.6 \text{ Hz}$ ,  $\text{CF}_3$ ), 126.1 (Dipp-*m*-CH), 126.5 (Dipp-*i*-C), 132.6 (Dipp-*p*-CH), 145.4 (Dipp-*o*-C), 175.5 ( $\text{C}_{\text{CAAC}}$ ).  $^{19}\text{F}$  NMR (376 MHz,  $\text{CDCl}_3$ , 297 K):  $\delta = -77.9$ .

### Data availability

Crystallographic data for this paper (CCDC 2245611–2245613, 2267007, 2267374) are available free of charge via the Cambridge Crystallographic Data Centre. Non-crystallographic data are provided in the Supplementary information file.

**Acknowledgements** This work was supported by the NSF (grant no. CHE-2246948). We thank A\*STAR for a postdoctoral fellowship for Y.K.L. We acknowledge the scientific support and HPC resources provided by the Erlangen National High Performance Computing Center (NHR@FAU) of the Friedrich-Alexander-Universität Erlangen-Nürnberg (FAU). The hardware is funded by the German Research Foundation (DFG). We thank F. F. Mulks for helpful discussions.

**Author contributions** Y.K.L. conceived and performed the synthetic experiments. M.M. and M.G. performed the X-ray crystallographic analyses. D.M. performed the computational work. G.B. supervised the project. The manuscript was written by Y.K.L., M.M. and G.B.

**Competing interests** The authors declare no competing interests.

### Additional information

**Supplementary information** The online version contains supplementary material available at <https://doi.org/10.1038/s41586-023-06539-x>.

**Correspondence and requests for materials** should be addressed to Ying Kai Loh or Guy Bertrand.

**Peer review information** *Nature* thanks the anonymous reviewers for their contribution to the peer review of this work. Peer reviewer reports are available.

**Reprints and permissions information** is available at <http://www.nature.com/reprints>.